Fundamental Research 4 (2024) 471–483

Contents lists available at ScienceDirect

Fundamental Research

journal homepage: http://www.keaipublishing.com/en/journals/fundamental-research/

Review

Laboratory studies on the infectivity of human respiratory viruses: Experimental conditions, detections, and resistance to the atmospheric environment

Yaohao Hu[a,b], Shuyi Peng[a,b], Bojiang Su[a,b], Tao Wang[a,b], Juying Lin[a,b], Wei Sun[a,b], Xiaodong Hu[a,b], Guohua Zhang[a,c], Xinming Wang[a,c], Ping'an Peng[a,c], Xinhui Bi[a,c,*]

[a] State Key Laboratory of Organic Geochemistry and Guangdong Provincial Key Laboratory of Environmental Protection and Resources Utilization, Guangzhou Institute of Geochemistry, Chinese Academy of Sciences, Guangzhou 510640, China
[b] University of Chinese Academy of Sciences, Beijing 100049, China
[c] Guangdong-Hong Kong-Macao Joint Laboratory for Environmental Pollution and Control, Guangzhou 510640, China

ARTICLE INFO

Article history:
Received 24 December 2022
Received in revised form 8 December 2023
Accepted 13 December 2023
Available online 21 February 2024

Keywords:
Respiratory viruses
Viral infectivity
Laboratory simulation
Atmospheric environmental condition
Airborne transmission

ABSTRACT

The environmental stability of infectious viruses in the laboratory setting is crucial to the transmission potential of human respiratory viruses. Different experimental techniques or conditions used in studies over the past decades have led to diverse understandings and predictions for the stability of viral infectivity in the atmospheric environment. In this paper, we review the current knowledge on the effect of simulated atmospheric conditions on the infectivity of respiratory viruses, mainly focusing on influenza viruses and coronaviruses, including severe acute respiratory syndrome coronavirus 2 and Middle East respiratory syndrome coronavirus. First, we summarize the impact of the experimental conditions on viral stability; these involve the methods of viral aerosol generation, storage during aging and collection, the virus types and strains, the suspension matrixes, the initial inoculum volumes and concentrations, and the drying process. Second, we summarize and discuss the detection methods of viral infectivity and their disadvantages. Finally, we integrate the results from the reviewed studies to obtain an overall understanding of the effects of atmospheric environmental conditions on the decay of infectious viruses, especially aerosolized viruses. Overall, this review highlights the knowledge gaps in predicting the ability of viruses to maintain infectivity during airborne transmission.

1. Introduction

Respiratory viruses generally infect epithelial cells of the human respiratory system and cause lesions in the respiratory tract. They mainly include the related viruses that cause epidemic outbreaks, such as severe acute respiratory syndrome coronavirus 2 (SARS-CoV-2), severe acute respiratory syndrome coronavirus (SARS-CoV-1), Middle East respiratory syndrome coronavirus (MERS-CoV), and pandemic influenza A virus (H1N1pdm09), and common respiratory viruses, such as seasonal influenza viruses, human rhinovirus (HRV), respiratory syncytial virus (RSV), and human seasonal coronaviruses (e.g., HCoV-229E and HCoV-OC43). Viral respiratory infections have caused serious harm to human health. A systematic analysis for the Global Burden of Disease Study showed that RSV and influenza viruses were two important causes of death from lower respiratory tract infection in 2016, of which 54% of the deaths due to RSV occurred in children under 5 years old [1]. It is estimated that there are up to 645,000 deaths related to respiratory infection caused by seasonal influenza worldwide each year [2]. Coronavirus disease 2019 (COVID-19) caused by SARS-CoV-2 has become a major public health emergency and has received wide concern since December 2019 (https://covid19.who.int), leading to > 507,000 published articles in the Web of Science dataset. At present, SARS-CoV-2 variants with stronger transmission are still emerging, posing a great challenge to the widespread implementation of effective treatments or vaccines. The transmission of respiratory viruses and their environmental stability need to be more clearly understood to formulate effective epidemic prevention and control measures.

The effective transmission of respiratory viruses between the infected individual and the potential host requires that the viruses maintain infectivity. Increasing evidence indicates the significant roles of aerosols and contaminated fomites (surfaces) in SARS-CoV-2 transmission [3,4]. Similarly, several studies have reported the presence of RNA of other respiratory viruses in ward air and on different surfaces, thus highlighting the risk of viral transmission by aerosols and fomites [5–8].

* Corresponding author.
E-mail address: bixh@gig.ac.cn (X. Bi).

https://doi.org/10.1016/j.fmre.2023.12.017

However, viable and dead viruses cannot be distinguished by nucleic acids present in the environment. The scientific brief from the World Health Organization also stressed the necessity to recover infectious viruses from air or surfaces, not just viral RNA, to accurately identify the routes of SARS-CoV-2 transmission [9].

Epidemiological and laboratory studies have shown that the transmission of viruses can be affected by atmospheric environmental conditions, such as temperature, relative humidity (RH), ultraviolet radiation (UV), and ozone [4,10]. However, there is still an evident gap in recognizing the mechanisms of infectious virus transmission, especially airborne transmission. Generally, epidemiological studies need to quickly identify the relationship between the levels of outbreak and some factors of concern, such as atmospheric environmental conditions (e.g., temperature, RH, and air pollutants). These efforts contribute to the formulation of policies to mitigate the pandemic. However, the relationship between atmospheric environmental conditions and the spread of COVID-19 is highly controversial according to our previous study [11]. This is mainly attributed to the complicated impact of atmospheric conditions on the pandemic in the real world. Comparatively, laboratory simulation studies need to explore the survival and decay of infectious viruses under controlled conditions, which is very important for epidemiological analysis and risk modelling [12,13]. Laboratory studies on the infectivity of coronaviruses and influenza A viruses (IAVs) on different surfaces and/or aerosols have been reviewed [14–18]. These viruses were reported to survive from hours to days on different surfaces. Recently, a critical review emphasized that differences in experimental conditions can lead to different outcomes in the inactivation of viruses by ozone [19]. In addition, studies have inferred that viral infectivity is significantly lost during sampling [20,21], thus impeding accurate assessment of the viral infectivity in the ambient environment. Therefore, technologies and conditions applied in simulation studies need to be carefully evaluated to further understand the impact of atmospheric environmental conditions on pandemic events.

Here, we review laboratory studies since 1960 on the stability of human respiratory viruses in aerosols or on surfaces. We aim to provide guidelines for studying the environmental stability of infectious respiratory viruses. First, the advances and limitations of the experimental techniques on viral infectivity are introduced; these include the generation, storage, and collection of viral aerosols as well as the other experimental settings. Second, the detection methods for measuring or quantifying the infectivity of viruses are reviewed; these include culturing in cells or tissue, nucleic acid-based and immunoassay-based analyses, and optical techniques. Finally, this review integrates the effects of atmospheric environmental conditions on viral infectivity, and further research directions are recommended.

2. Effects of experimental conditions on viral infectivity in laboratory studies

The aerosol generation, ageing, and collection techniques and their ability to maintain the infectivity of respiratory viruses are introduced in the first three subsections. The effects of experimental conditions on the stability of viruses deposited on the surface are discussed in the last subsection.

2.1. Artificial generation of viral aerosols and its impact on viral infectivity

2.1.1. Nebulizers for viral aerosol generation

Reflux nebulizers are mostly used for viral aerosol generation (Tables 1 and S1). Among them, 3-jet and 6-jet Collison nebulizers are widely used in the nebulization of respiratory viruses, including SARS-CoV-2, SARS-CoV-1, MERS-CoV, HCoV-229E, influenza viruses, and rhinovirus. Some studies hypothesized that refluxing nebulized viruses may produce reduced infectivity due to strong collisions, shearing forces, and recycling [22,23]. In contrast, nonreflux nebulizers enable the suspensions to pass through the nozzle only once, do not need more collisions and require lower pressure; thus, these nebulizers can possibly reduce damage to the viruses and effectively maintain viral infectivity [24].

Several studies have reported that viruses are always less infectious in aerosols than in suspensions within the nebulizer. Fears et al. [25] reported extremely low spray factors (SFs, the ratio of viral titre in aerosol to the initial titre in the suspension) yielded by 3-jet and 6-jet Collison nebulizers and an Aerogen Solo nebulizer for SARS-CoV-2, SARS-CoV-1, and MERS-CoV, and the SFs ranged from −6 to −5.3 $\log_{10}$. Similarly, the nebulization efficiency of the Collison nebulizer was also very low for influenza viruses, SARS-CoV-2, or MERS-CoV, with SFs of approximately −3 to −2 $\log_{10}$ [26–29]. Niazi et al. [30] reported that the SFs of two influenza A viruses and human rhinovirus 16 post-nebulization ranged from 0.5 to 0.8; however, the sample concentration used to calculate these SFs was not converted to a volume concentration unit in aerosol. Increasing the initial load of infectious viruses could improve the survival of the viruses in aerosols [31].

The composition of the suspension is critical for the stability of viral infectivity in aerosols. The components encapsulating the particles may protect the virus from the surrounding environment, thus maintaining viral infectivity. Organics in suspension have been found to protect bacteriophages PR772 and Φ6 from nebulization and sampling [23]. The bacteriophage MS2 survived better in protein-rich tryptic soy broth than in salt-rich artificial saliva without mucin after nebulization [32]. Compared with the medium with 10% synthetic tracheal mucus, the infectivity of the influenza viruses in the medium with 10% bovine pulmonary surfactant had a greater loss of 2–4 $\log_{10}$ $TCID_{50}$/mL after nebulization, potentially due to the interaction between the surfactant and the lipid membrane of the virus, thus reducing viral infectivity [33].

2.1.2. Size of viral aerosols

The size of viral aerosols plays an important role in the airborne transmission of respiratory viruses. The ferret model shows that the effective spread of influenza viruses is associated with the release of submicron aerosols [34]. Droplets produced by speech, coughing, and sneezing vary in size from less than 1 μm to up to 2×10^3 μm [35]. However, micron or submicron particles are dominant in the quantity of exhaled droplets. Wang et al. [4] showed that exhaled aerosols exhibited a multimodal size distribution with peak values at 0.1 μm, 0.2–0.8 μm, 1.5–1.8 μm, and 3.5–5.0 μm, depending on the generation locations, processes, and respiratory activities. Noti et al. [36] found that the fastest decay of viral infectivity occurred at a size of > 4 μm (which led to 90% loss in infectivity), while only 29% loss occurred at a size of 1–4 μm after 15 min of nebulization. They attributed the larger loss in viral infectivity to the higher sedimentation rate of the larger particles.

Once released to the ambient dry air, the droplets will undergo rapid dehydration and equilibrium to a stable particle size. The larger particle size of 100 μm could shrink to ~30 μm in only 20 s when exposed to 55% RH, while the released particles with smaller initial diameters (2–10 μm) could reach their equilibrium size almost instantaneously (0.01–0.1 s) [37]. Using a model based on Köhler theory, Yang et al. [38] calculated that a particle of 10 μm containing saliva-like composition could shrink to 24% of its initial size at 90% RH and to 17% of that at 60% RH, which could lead to an increase in the pH in droplets. This consequence probably further caused conformational changes in the glycoproteins on the viral envelope, thereby reducing its infectivity. In another study, Yang and Marr [35] modelled the size distribution and dynamics of influenza viruses emitted by coughing at 10%–90% RH and observed the increased removal of viable influenza viruses at higher RH.

2.2. Aerosol chambers used in the decay simulation of viral infectivity

Decay tests of viral infectivity are generally conducted in an aerosol chamber under controlled conditions. Several bioaerosol chambers (such as static, flow-through, and rotating chambers and microthread

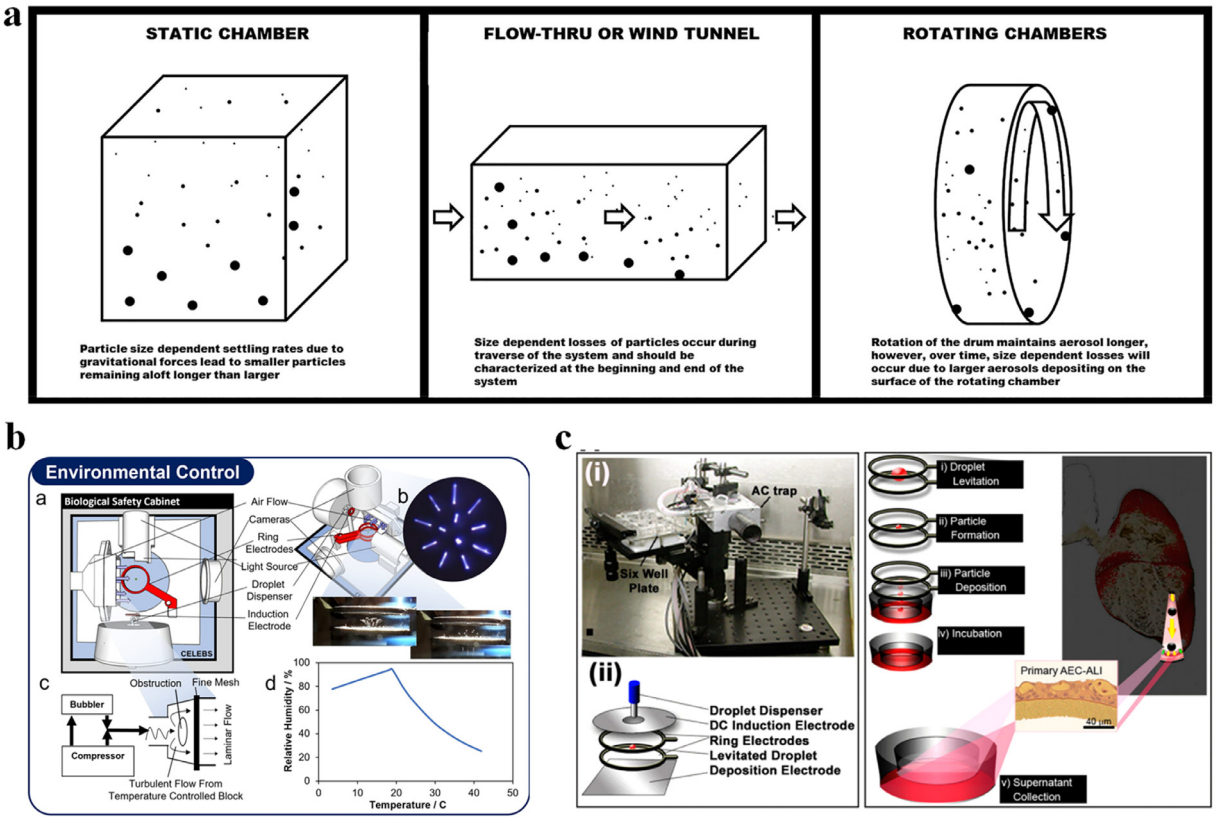

Fig. 1. Testing system for studies on viral infectivity in aerosols. (a) Traditional bioaerosol control system including static, flow-through, and rotating chamber (from left to right). Image a reprinted with permission from Santarpia et al. [39]. Copyright 2019 Taylor & Francis Ltd. (b) and (c) Schematic diagrams of CELEBS and the double-ring control of droplet suspension and deposition, respectively. Image b reprinted with permission from Oswin et al. [53]. Copyright 2021 Taylor & Francis Ltd. Image c reprinted with permission from Cruz-Sanchez et al. [51]. Copyright 2013 American Chemical Society.

systems) have been introduced in several reviews [39,40]. In this subsection, the aerosol chambers used for respiratory viruses are reviewed (Fig. 1).

2.2.1. Static and flow-through chambers

Static chambers are often used in studies that only require aerosol mixing without long-term suspension, for example, to determine the performance of different nebulizers or the short-term stability of the viruses through a phase transition from liquid to aerosol. The sizes of the static chambers range from a few litres to dozens of square metres. Gravity settlement is inevitable for static chambers [41,42]. Moreover, as mentioned in Section 2.1.2, RH could affect the size of aerosols and further the sedimentation rate. Therefore, the physical loss under different RH values needs to be corrected when using static chambers.

Flow-through chambers are mainly used for buffering or mixing of continuous input aerosols. Different from static chambers, the driving force of aerosols in the flow-through chambers is the pressure caused by flow velocity rather than gravity; thus, their application is more flexible. For example, Ratnesar-Shumate et al. [43] tested the collection efficiency of eight samplers for airborne SARS-CoV-2 infectivity using a flow-through chamber (aerosol test plenum) with multiple sampling ports. Zupin et al. [31] built an aerosol test system containing a circular transport pipe (aerosol transmission tube) with a length of 30 cm and a diameter of 7.5 cm to evaluate the infectivity of SARS-CoV-2 in aerosols. In principle, the length of the flow-through chambers along with the direction and speed of the airflow in the chambers could be changed to study the hydrodynamics of viral aerosols. However, the physical loss caused by the increased length of the chamber needs to be reevaluated [39].

2.2.2. Rotating chambers

Rotating chambers based on the original design of the Goldberg drum have been widely used in studies on the decay of infectivity of viral aerosols. Compared with static chambers, rotating chambers can increase the residence time and reduce the physical loss caused by aerosol gravity sedimentation and diffusion. For example, approximately 30% of infectious rhinoviruses and 20% of influenza viruses can be detected in Goldberg drum even after 23–24 h of nebulization [44,45]. At present, optimized rotating chambers vary from 10 L to 2000 L and have been developed to investigate the effect of the physical parameters of the particles and environmental factors, such as temperature, RH, sunlight, and ozone, on the viral infectivity [25,29,33,46,47]. Additionally, the optimized rotational speed of the rotating chamber can improve the suspension time for different particle sizes [48]. To minimize losses of aerosol in the chamber, a rotational speed of 1–4 rpm is used in most rotating chambers.

The decay rate of the viral aerosol in the rotating chamber can be calculated by the first-order decay kinetics (Eq. 1).

$$C = C_0 \times e^{-k_1 t} \quad (1)$$

where C is the concentration of the infectious virus at sampling time t, C_0 is the initial concentration of the infectious virus, and k_1 is the decay rate constant. The decay constant k_1 consists of $k_{physical}$ and $k_{biological}$, which represent losses caused by physical processes (such as natural settlement in the chambers, wall loss, and loss during sampling) and loss of viral infectivity during sampling, respectively [47,49,50].

2.2.3. Controlled electrodynamic levitation and extraction of bioaerosol onto a substrate (CELEBS)

Generally, artificially generated aerosols are polydisperse in physical and chemical properties. The development of single-particle suspension

and analysis techniques can aid in the explanation of the relationship between microenvironmental heterogeneity and the biological decay of single bioaerosol droplets [39,40]. Nevertheless, the applications of single-particle suspensions and analytical technologies in the bioaerosol field are still limited.

In recent years, electrodynamic equilibrium techniques, which can form an electrodynamic trap that restricts a single aerosol particle to a fixed position stay for several days (Fig. 1b, 1c), have been applied to study the infectivity of individual virus-laden particles. Using an electrodynamic trap, Cruz-Sanchez et al. [51] studied the direct effect of the interaction between the particulate matter and RSV on airway epithelial cells. Later, a similar method, known as controlled electrodynamic levitation and extraction of bioaerosol onto a substrate (CELEBS), was introduced and applied to study the aerosol activity of bacteria (Escherichia coli and Bacillus) [52] and mouse hepatitis virus [53]. The integrated design of the CELEBS could minimize the disadvantages of the Goldberg drum, such as the impact of aerosol production and sampling processes.

2.3. Collection of the viral aerosols

Bioaerosol samplers have been widely used in the study of pollens, bacteria, and fungi, but these technologies still have challenges in the collection of viral aerosols [21,54]. The collection efficiency of the samplers, determined by physical collection efficiency and biological collection efficiency, is critical for accurately calculating the attenuation of infectious viruses in the air. This section mainly focuses on the sampling technologies for airborne respiratory viruses (Fig. 2). Table S2 presents the advantages and disadvantages of the sampling mechanisms for maintaining viral infectivity.

2.3.1. Impactors and cyclones

Impactors are active samplers that use a vacuum pump to inhale aerosol particles and accelerate them through the nozzle. The particles hit the collection medium due to inertia; thus, the smaller particles with less inertia can easily follow the streamline. The physical collection efficiency of the impactors depends on the diameter and density of particles as well as the velocity and diameter of the nozzle [55]. Impactors are usually used to capture large bioaerosols, such as bacteria and fungi. The cascade impactor can separate aerosol particles into different size fractions, which can aid in the understanding of the difference in viral infectivity among different particle sizes. Using a personal cascade impactor sampler (Sioutas), Lednicky et al. [56] analysed the infectivity of influenza viruses in five particle size ranges and found that ultrafine aerosol particles contained viable viruses.

Similar to impactors, the impact of traditional cyclones usually depends on high flow rates (tens to hundreds of lpm), causing difficulty to maintain viral infectivity. A portable two-stage cyclone developed by the National Institute for Occupational Safety and Health (NIOSH) consists of two 1.5 mL centrifuge tubes, enabling low flow operation [57]. This improved sampler can collect two particle sizes (> 4 μm and 1–4 μm) into two disposable centrifuge tubes and a particle size of < 1 μm onto a polytetrafluoroethylene (PTFE) filter at a low flow rate (3.5 lpm). Using three-stage NIOSH cyclones, Noti et al. [58] found that most of the particles containing infectious influenza viruses exhaled by simulated cough were < 4 μm (5.0% in > 4 μm, 75.5% in 1–4 μm, and 19.5% in < 1 μm). However, the infectivity of the SARS-CoV-2 Delta variant could not be recovered by cyclones in the air [59]. This was potentially due to unavoidable long-term sampling, which aggravated the loss from the sampler wall and drying process. For example, using the SKC BioSampler as the reference sampler, the ability of the NIOSH sampler to maintain infectivity was 35% (sampling time of 15 min), 28% (30 min), and 15% (60 min) of that of the SKC BioSampler [60].

2.3.2. Liquid impingers

Liquid impingers have been widely used as reference samplers in studies of viral infectivity. This is a gentler sampling method for viruses than solid surface impaction; thus, the viral infectivity is well preserved. There are two commonly used liquid impingers: all-glass impingers (AGIs) and SKC BioSampler. Generally, AGI has only one nozzle that can reach sound speed. The large particles passing through the nozzle collide with the liquid due to inertia, and the resulting bubbles aids in the collection of small particles [20]. AGI has mostly been used in early studies on viruses, including MERS-CoV, rhinovirus, HCoVs, and influenza viruses [41,44,45,61,62].

SKC BioSampler exhibits better performance in the recovery of infectivity. It has several nozzles of 0.66 μm; these improve the aerosol collection mainly through combined impact and centrifugal motion (eddy motion). Using the SKC BioSampler, researchers have successfully recovered viable influenza viruses from coughs and exhalations of patients and from air in isolation wards [63,64]. Compared with other samplers, such as the compact cascade impactor (CCI), Teflon filters, and gelatine filters, the SKC BioSampler showed the highest recovery rate of infectious viruses (75%–110% vs. 7%–22%) [65]. However, the

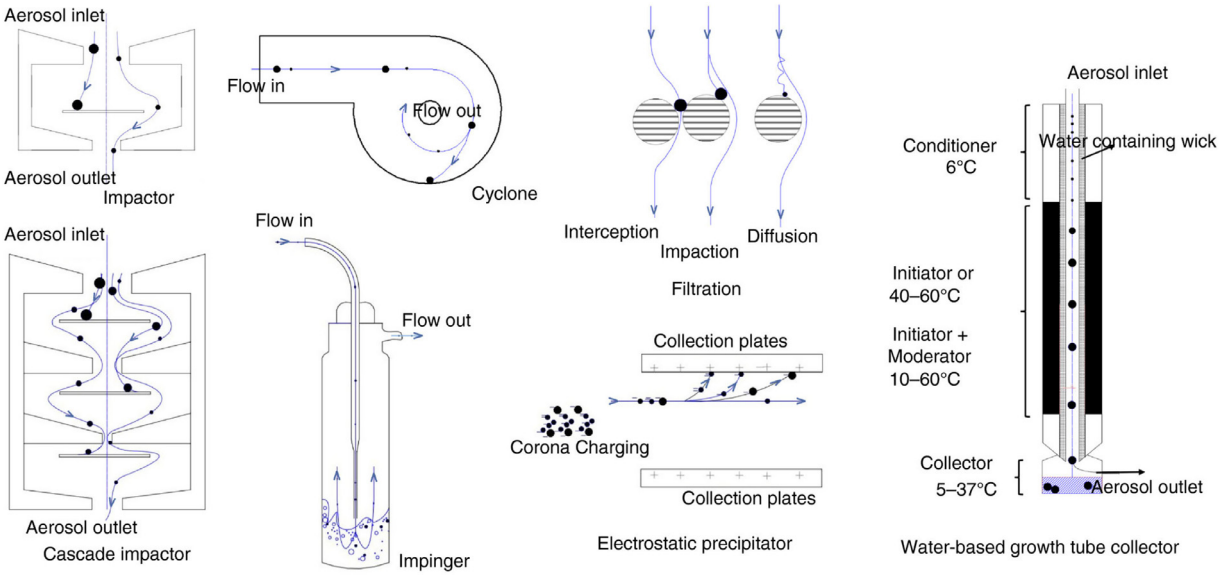

Fig. 2. Various samplers used for collecting viral aerosols. Image reprinted with permission from Pan et al. [21]. Copyright 2019 John Wiley & Sons, Inc.

SKC BioSampler was less efficient at collecting submicron and ultrafine virus aerosols, with a recovery of only 10%–50% [66,67].

2.3.3. Filter-based samplers

Filter-based samplers collect aerosols onto different filters based on interception, inertia, diffusion, and electrostatic attraction [20]. PTFE collected particles with a size of 100–900 nm and a collection efficiency of > 93% for airborne phage MS2; polycarbonate (PC) filters had lower physical collection efficiencies of only 49% and 22% for particles of 47 nm and 63 nm, respectively [68]. Gelatine filters had a physical collection efficiency of ~100% for influenza viruses in aerosols with a size of 20–300 nm. Similarly, the glass fibre filter also showed a physical collection efficiency of 100% for particles in the range of 30 to 300 nm [67].

However, filters generally have very low efficiency in infectious virus collection [67]. Agar and semisolid gelatine filters were found to be more effective than virus transport medium (VTM) in biological recovery [69]. Compared with other filters, gelatine filters have unique advantages: they are easy to dissolve in liquid and do not affect the subsequent detection of infectivity; thus, they are widely used in laboratory studies on the ageing of infectious respiratory viruses (Table 1). Gelatine filters have been successfully used to collect viable SARS-CoV-2 [70] and MERS-CoV from the air of the isolation ward of patients [6]. However, long-term sampling in ambient air remains challenging in the recovery of viral infectivity because of the effects of drying [71].

2.3.4. Emerging sampling technologies

Traditional samplers (impactors, impactors, and filters) are often accompanied by inefficient collections of fine particles, virus dehydration, or wall loss. To overcome these shortcomings, some new sampling technologies have emerged. For example, growth tube collector technology (GTC, also known as viable virus aerosol sampler (VIVAS)) can be used to effectively collect fine particles and maintain better viral infectivity [72,73]. Recently, Vass et al. [59] successfully detected viable SARS-CoV-2 Delta variants in aerosol samples using commercial BioSpot-VIVAS. Another new sampling technology beneficial to the maintenance of viral infectivity is the electrostatic precipitator (ESP), in which incoming particles are charged and transferred to the collection medium by electrostatic attraction or repulsion. The currently developed ESP can collect monodisperse polystyrene particles of 0.05–2 μm with recoveries of 99.3%–99.8% [74]. This method has been successfully used in the collection of viable SARS-CoV-2 in indoor air [75]. The advantage of ESPs is that their impact on bioaerosol particles is low [54], and its disadvantage is that ozone and reactive oxygen species (ROS) produced by corona discharge can inactivate viruses. However, the addition of the ROS scavengers such as ascorbic acid to the collection medium (phosphate-buffered saline) can effectively alleviate this effect [76,77].

2.4. Laboratory simulation of viral stability on surfaces

The steps to study the stability of viruses deposited on different surfaces generally include inoculation, exposure, and recovery for further detection in laboratory simulations. Notably, several factors, such as virus types and strains, suspension matrixes, initial inoculation volumes and concentrations, and droplet drying, could lead to different results among the studies.

2.4.1. Virus types and strains

Different virus types known for their different virus structures show different decay patterns of infectivity [17,61,78]. Whether in plastic, stainless steel, glass, or skin, SARS-CoV-2 always survived longer than IAV [78]. van Doremalen et al. [61] found that viable MERS-CoV could be recovered from stainless steel and plastic surfaces at 48 h after inoculation, while influenza H1N1 viruses were not able to be detected at 4 h. Even for coronavirus, the stability of different genera on the surfaces was also different. Most studies have shown that *β-coronaviruses* (SARS-CoV-2, SARS-CoV-1, and MERS-CoV) have relatively high stability on surfaces such as polypropylene, stainless steel, copper, cardboard, and glass [61,79,80]. However, HCoVs, which belong to *α-coronavirus*, are less stable on surfaces. Rabenau et al. [81] found that the stability of SARS-CoV-1 on polypropylene was better than that of HCoV-229E. HCoV-229E was found to survive ~3 h on aluminium, sterile latex surgical gloves, and aseptic sponges [82].

Identifiers of influenza virus strains used in this review are listed in Table S3. Most studies have shown that IAVs (A/H1N1pdm, A/NC-H1N1, and A/Brazil-like H1N1) tend to be more stable than IBVs (IBV-Texas, IBV-Illinois-like, and IBV-HK) under 30%–55% RH [83–85]. Among the subtypes of IAVs, H1N1 (A/NC-H1N1) can survive for only 1 h, while H3N2 (A/Wis-H3N2) can survive for 3 days [83]. For different strains of H1N1, significant differences in the stability of the A/New Caledonia/20/1999 strain (H1N1) and A/Brisbane/59/2007 (H1N1) on stainless steel were observed. The difference in stability between the different viral strains was potentially attributed to slight changes in the composition of fatty acids in the outer phospholipid membrane of the influenza virus [86].

2.4.2. Suspension matrixes

A culture medium or VTM is often used for virus extraction, preservation, and suspension on surfaces. To simulate respiratory fluids, natural or artificial saliva and mucus are used as organic substrates to suspend the viruses. As early as the 1940s, the protective effect of human mucus on the survival of influenza viruses was mentioned [87]. Yang et al. [88] investigated the effects of protein, salt concentration, and mucus on the stability of influenza H1N1 viruses at ~50% RH. They found that viral infectivity decreased by ~2 $\log_{10}$ in a salt solution and the loss increased with increasing salt concentration, while no significant loss occurred after the addition of protein to the solution.

Artificial saliva or mucus is also widely used in the study of SARS-CoV-2 [89–92]. It was reported that SARS-CoV-1 was protected in suspension with 10% fetal calf serum [81]. In a suspension with 10 g/L bovine serum albumin, the stability of SARS-CoV-2 significantly increased (from 48 h to > 96 h) on the surface of glass [93]. Compared with the culture medium, the addition of artificial mucus and protein significantly increased the resistance of SARS-CoV-2 to inactivation under simulated sunlight (1.28 W/cm^2 UVB) [89,94]. However, Ratnesar-Shumate et al. [95] showed that the addition of artificial saliva significantly accelerated the decay of SARS-CoV-2. IAV deposited on common surfaces (stainless steel/glass/plastic) was inactivated faster in natural mucus (from sputum samples) than in the culture medium [78]. Overall, the impact of the suspension on viral infectivity remains contentious until now.

2.4.3. Inoculum volumes and titres

Human respiratory activities, such as breathing, talking, coughing, and sneezing, can emit a series of droplet sizes (see 2.1.2). Therefore, studies on the relationship between droplet sizes deposited on surfaces and the decay of viral infectivity can aid in the understanding of the behaviour of viruses in transmission by fomites. The inoculum volumes of suspensions containing viruses exceeded three orders of magnitude from 0.1 μL to 500 μL in previous studies. The most commonly used volume was 5–50 μL. Droplet size on the fingers has been shown to have a direct effect on the stability of influenza viruses, and a larger droplet size may provide a beneficial microenvironment to protect the viruses [96]. A recent study on the effect of inoculation volume (1 μL, 5 μL, and 50 μL) showed that different initial droplet volumes affected the time for droplets to reach quasi-equilibrium and led to various environmental stabilities of the enveloped viruses [97]. However, Biryukov et al. [92] found that inoculum volumes (1 μL, 5 μL, and 50 μL) did not affect the stability of SARS-CoV-2 deposited on stainless steel.

Table 1
Experimental conditions and estimated half-lives of viral infectivity on artificially aerosolized human respiratory viruses under different temperatures (Temp.) and relative humidity (RH) in darkness.

Study	Virus	Conditions				Temp. (°C)	RH (%)	k_1 (min)	K (lg/h)	$Rt_{1/2}$ (h)	R^2
		Nebulizer	Particle size	Sampler	Matrix						
(Schuit et al., 2021) [124]	SARS-CoV-2	Air assist nozzle	MMAD: 2 μm	Gelatine filter	sRTLF	20	20–70	0.005		2.31	
						40	20	0.012		0.96	
						10	70	0.001		11.55	
						30	70	0.029		0.40	
(Dabisch et al., 2021) [49]	SARS-CoV-2	Air assist nozzle	MMAD: 1.94 μm	Gelatine filter	Simulated saliva	10	70	0.018		0.64	
						20	20	0.006		1.93	
						20	70	0.017		0.68	
						30	70	0.066		0.18	
						40	70	0.04		0.29	
(Smither et al., 2020) [26]	SARS-CoV-2	Collison nebulizer (3-jet)	Size: 1–3 μm	Impinger	DMEM	20	50	0.009		1.27	
						20	78	0.016		0.7	
					Artificial saliva	20	50	0.023		0.51	
						20	78	0.004		2.9	
(Schuit et al., 2020) [47]	SARS-CoV-2	Air assist nozzle	MMAD: 1.78 μm	Gelatine filter	Artificial saliva	20	20–70	0.008		1.44	
			MMAD: 1.88 μm	Gelatine filter	CM (with 10% FBS)	20	20–70	0.013		0.89	
(Schuit et al., 2019) [50]	A/PR8-H1N1	Ultrasonic nozzle	MMAD: 4.1–4.4 μm	Gelatine filter	CM (with 8% FBS)	20	20, 70	0.02		0.58	
(van Doremalen et al., 2020) [79]	SARS-CoV-2	Collison nebulizer (3-jet)	Size: < 5 μm	Gelatine filter	CM (with 2% FBS)	22	65			**1.09**	
	SARS-CoV-1					22	65			**1.18**	
(Pyankov et al., 2018) [27].	MERS-CoV	Collison nebulizer (3-jet)	Size: 0.7–1.8 μm	Personal sampler	CM (with 2% FBS)	25	79		0.284	1.06	(0.90)
						38	24		0.572	0.53	(0.99)
(Pyankov et al., 2012) [28]	A/H1N1pdm	Collison nebulizer (3-jet)	Size: 0.5–2 μm	Personal sampler	DMEM	25	55		0.767	0.39	(0.96)
	A/Aichi-H3N2					25	55		0.220	1.37	(0.95)
(Karim et al., 1985) [44]	Rhinovirus-14	Collison nebulizer (6-jet)	Size: <5 μm	All-glass impinger	TPB	20	80			**13.7**	
(Ijaz et al., 1985) [125]	Human Coronavirus 229E	Collison nebulizer (6-jet)	NP	NP	TPB	20	30			**26.76**	
						20	50			**67.33**	
						20	80			**3.34**	
						6	30			**34.46**	
						6	50			**102.53**	
						6	80			**86.01**	
(Rechsteiner and Winkler, 1969) [46]	Respiratory syncytial virus	FK 8 direct type atomizer	MPS: 4.9 μm	Impinger	Distilled water	20.5	20		0.500	0.60	
						20.5	30		1.070	0.28	
						20.5	40		0.590	0.51	
						20.5	50		0.770	0.39	
						20.5	60		0.700	0.43	
						20.5	70		1.470	0.20	
						20.5	80		2.200	0.14	
						20.5	90		1.720	0.18	
(Harper, 1961) [45]	A/PR8-H1N1	Collison atomizer	NP	Impinger	McIlvaine's buffer (with 0.2% casein)	7.5	24		0.023	13.20	(0.95)
						7.5	51		0.023	13.38	(0.87)
						7.5	82		0.066	4.55	(0.97)
						22.25	21		0.022	13.50	(0.92)
						22.25	35		0.032	9.44	(0.92)
						22.25	50.5		0.213	1.41	(0.96)
						22.25	64.5		0.198	1.52	(0.90)
						22.25	81		0.168	1.79	(0.79)
						32	20		0.075	4.04	(0.96)
						32	49.5		0.311	0.97	(0.94)
						32	81		1.093	0.28	(0.95)

Notes: MMAD: mass median aerodynamic diameter; MPS: mean particle size; sRTLF: simulated respiratory tract lining fluid; CM: culture medium; TPB: tryptose-phosphate broth; NP: not pointed out in the original literature. Recalculated half-lives ($Rt_{1/2}$) in this paper are identified by the corresponding R^2 value in parentheses. The value of $Rt_{1/2}$ in bold represents the reported half-lives derived from the original papers. k_1 is given in loss of titre ($TCID_{50}$/mL or PFU/mL) per min and K in log_{10} titre loss per hour, which can be converted to $Rt_{1/2}$.

The initial inoculum titres of the viruses may also affect the stability of the deposited viruses. The stability of the A/Mos-H3N2 viruses deposited on banknotes increased from 1 h to 2 days as the initial titre increased 8 times [83]. Similarly, the recovery of parainfluenza virus was enhanced when the viral load increased from 1 to 3 $\log_{10}$ $TCID_{50}$/mL [98]. van Doremalen et al. [79] found that culture medium-suspended SARS-CoV-2 could survive for 3 days on stainless steel using an initial titre of 5 $\log_{10}$ $TCID_{50}$/mL, while Chin et al. [99] and Riddell et al. [91] found that it could survive for nearly 7 days using an initial load of 7–8 $\log_{10}$ $TCID_{50}$/mL.

2.4.4. Drying of droplets

Viral droplets gradually dry when inoculated on surfaces due to the unsaturated RH of the surrounding environment. At present, the studies can be divided into two groups: one is to observe the dry virus (after drying), and the other is to observe the wet virus (immediately after inoculation). Dried SARS-CoV-1 and SARS-CoV-2 have shown survival on the surface for several days [100–102]. For wet viruses, Firquet et al. [103] found that the decay of wet viruses significantly increased with increasing drying times. A recent study used a microbalance to observe the stability of SARS-CoV-2 and found that there was no significant change in the titre of the virus on the surface before the droplets were completely dried [104]. However, the viral titre began to decrease once efflorescence occurred. Similar results were found in earlier studies in which wet parainfluenza viruses were more stable on both nonabsorptive and absorptive surfaces than dry viruses [98]. Overall, the main decay of the virus occurs in the process of droplet drying, not after drying.

Notably, the drying time is dependent on the inoculation volumes. The drying of 50 μL droplets on polystyrene takes 10 h at 22°C and 65% RH [104], while the drying of 1 μL droplets only takes 1 h at 22°C and 75% RH [105]. These differences cause great difficulty in the differentiation of the dynamic decay of viruses in many laboratory studies. Additionally, the composition of the suspension may also affect the sensitivity of different viruses to inactivation during drying [90,95,106,107].

3. Detection and evaluation methods for the viral infectivity in environments

The methods for detecting viral infectivity in environmental samples reviewed in this section include conventional and potential methods such as culturing-, nucleic acid-based analysis, immunoassay, and optical techniques. Table 2 summarizes the advantages, disadvantages, and applications of these detection methods.

3.1. Traditional culturing in cells or tissues

The culture method is the gold standard for determining viral infectivity, which is mainly measured by observing the number of plaques and cytopathic effects (CPE). Plaque-forming units (PFUs) were used to quantify the viral titre. Usually, a series of 10-fold diluted viruses is inoculated into each plate to infect cells and then the cells were cleaved and release more viruses to infect the neighbouring cells. As the infection repeats, the infected area forms a visible plaque [108]. This method is limited to some viruses such as influenza viruses that induce cell lysis or death and form plaques on the cell monolayer in the cell culture plate; however, many viruses do not form plaques and only induce recognizable CPE [109]. The end-point dilution method was used to quantify the effects of the 10-fold diluted viruses added to the cell monolayer, and the viral dilution in 50% of cells with CPE (tissue culture infective dose 50%, $TCID_{50}$) was determined after a few days [110]. However, viral detection using culturing methods still has great challenges because of the low recovery of infectious viruses in real environment.

3.2. Nucleic acid-based analysis

Viral nucleic acid as a genetic material has been a routine index for the detection and identification of viruses. Reverse transcription quantitative polymerase chain reaction (RT–qPCR) is widely used to measure viruses in the environment. However, viral nucleic acids alone cannot indicate whether the virus present in the environment is infectious. Thus, optimized nucleic acid-based detection was developed. Nuanualsuwan et al. [111] considered that the capsid protein of the damaged virus was more easily degraded by protease than the unharmed capsid protein; thus, they added protease K and nuclease to eliminate the interference of the inactivated virus before RT–qPCR detection of the samples. Bonifait et al. [112] noted that the addition of propidium monoazide to the qPCR system could distinguish noroviruses with intact structure or membrane damage, thus reducing the detection of inactivated viruses during testing and eliminating false positives. A combination of a variety of conventional detection methods also enables the detection of viral infectivity, such as cell culture combined with qPCR (ICC–qPCR) or viral replication assay (VRA), cell culture combined with ELISA or fluorescence microscopy to detect antibodies [113].

3.3. Immunoassay

Immunoassays based on the specific combination of antigens and antibodies are widely used to detect the viability of pathogenic microorganisms [114]. Immunological techniques commonly used to detect viruses include enzyme-linked immunosorbent assay (ELISA), radioimmunoassay (RIA), and chemiluminescence immunoassay (CLIA) [115,116]. Based on the principle of immunology, biosensors have received extensive attention in the detection of viruses since they can improve the sensitivity of detection and reduce the sample size and cost [117]. At present, several types of low-cost and time-saving biosensors, such as electrochemical sensors, quartz crystal microbalances (QCMs), and field effect transistors (FETs), have been developed to quickly identify different viruses (Fig. S1). For example, a graphene-based FET biosensor developed by Seo et al. [118] could detect SARS-CoV-2 in clinical samples without extracting viral nucleic acids. The limit of the biosensor for real-time detection of SARS-CoV-2 was lower than 16 PFU/mL. However, the effectiveness of immunoassays for viral infectivity is still debateable. Indeed, false positives in immunoassays depend on the content of free proteins or damaged proteins around viruses and their binding ability to antibodies.

3.4. Optical techniques

With the development of imaging equipment and tuneable laser sources, optical tools are increasingly used in the detection of viral infectivity. Optical technologies include fluorescence microscopy, Fourier transform infrared spectroscopy (FTIR), and surface-enhanced Raman scattering (SERS) (Fig. S2). Noyce et al. [119] detected influenza H1N1 viruses with a fluorescein isothiocyanate-labelled antibody and measured the viral infectivity by fluorescence microscopy. Using FTIR, the absorption abundance at 1124 cm^{-1}, which reflected the phosphodiester-linked nature of RNA, was increased when Vero-E6 cells were infected by infectious SARS-CoV-2 rather than inactivated SARS-CoV-2 [120]. SERS can improve the measurement sensitivity of viral infectivity [121]. In addition, combining SERS with microfluidics can simultaneously measure the infectivity of several respiratory viruses, including rhinovirus, influenza viruses, and parainfluenza viruses, and their subtypes can be distinguished based on principal component analysis of the Raman scattering [122]. In the future, optical tools need to be developed with miniaturization and low cost to increase their usage in various applications.

Table 2
Detection methods of viral infectivity.

Classification	Methods	Advantages	Disadvantages	Comments	References
Cell culture	Plaque	◆ Distinguish the infectious viruses and dead viruses	◆ Specific culture conditions ◆ Time-consuming ◆ Low sensitivity		Rigotto et al. [136]
	$TCID_{50}$	◆ Distinguish the infectious viruses and dead viruses	◆ Specific culture conditions ◆ Cannot form significant cytopathic effects at low viral load		Agol [109]
Nucleic acid-based analysis	RT–qPCR	◆ Highly specific and sensitive when using primers ◆ Amenable to high-volume testing	◆ Specialized equipment required ◆ Fail to distinguish the infectious viruses and dead viruses		Liu et al. [137]
	RT–qPCR, nucleases, and reagent D	◆ Highly specific and sensitive and exclude dead viruses	◆ Specialized equipment required ◆ Depend on the viral load		Bhardwaj et al. [138]
	ICC–PCR	◆ Highly specific and sensitive and exclude dead viruses ◆ Developed commercial kits	◆ Specific culture conditions ◆ Cost-consuming ◆ Specialized equipment required ◆ Depend on the viral load	Lesser application to detection of respiratory viruses such as SARS-CoV-2 and influenza viruses	Rodríguez et al., [139]
Immunoassay	ELISA	◆ Highly sensitive and stable	◆ Cross-reactivity of antibodies to other co-infecting viruses ◆ False positives in the results		Pimenta et al. [115]
	CLIA	◆ Highly signal intensity and specificity ◆ Low consumption of reagents	◆ Closed analytical systems ◆ Limited tests panel ◆ False positives in the results		Li et al. [116]
	QCM, FET, and Electrochemical sensors	◆ Highly flexibility and sensitive ◆ Low-cost	◆ Specialized equipment required ◆ Less reproducibility and stability	Potential detection for viable viruses	Layqah and Eissa [140]
Optical techniques	Raman spectroscopy	◆ Distinguish different virus species based on Raman spectroscopy	◆ Specialized equipment required		Yeh et al. [122]
	Fluorescence-based virus detection	◆ Visualized the viral RNA/DNA using fluorescence technique	◆ Fluorescent labels are easily quenched		Noyce et al. [119]
	Fourier transform infrared	◆ Highly sensitive ◆ Visualized the absorption of aliphatic and saccharide in the cells	◆ Specialized equipment required		Kazmer et al. [120]

4. Environmental conditions affecting the infectivity of respiratory viruses

Since the outbreak of COVID-19, studies on the transmission of viruses in the environment have rapidly increased. Guillier et al. [123] and Morris et al. [104] conducted a meta-analysis of coronavirus inactivation by temperature and RH; however, most of their data came from viral inactivation in solutions. Here, we reviewed published results on the decay of respiratory viruses in aerosols and on surfaces (Tables 1 and S4). Studies on virus inactivation in solutions were excluded from our analysis.

Generally, the decay constant k_1, K ($\log_{10}$ $TCID_{50}$/mL loss per hour), half-life (the time to reduce viral infectivity by 50%, $t_{1/2}$), and D value (the time to reduce viral infectivity by 90%) are used to quantify the decay of the viruses. Here, we summarized half-lives or converted other parameters to half-lives ($Rt_{1/2}$) based on first-order decay kinetics. For studies that did not report the characteristics of viral decay, we used digitization tools in Origin 7.0 to manually extract and convert data ($\log_{10}$ titre vs. hours) from charts and record metadata involving virus types, inoculations, suspensions, surfaces, and environmental conditions. The charts used for extraction and the final dataset are available in a GitHub repository (https://github.com/YaohaoHu/Review-for-FR.git). Eq. 2 (logarithmic 10 transformation of Eq. 1) was used to recalculate the half-life ($Rt_{1/2}$), which is $\log_{10}2$ times the reciprocal of K (the absolute value of the slope in the linear regression). Data attaining $R^2 > 0.8$ in linear regression were recorded.

$$\log_{10}(C) = \log_{10}(C_0) - \frac{\log_{10}2}{Rt_{1/2}}t \quad (2)$$

4.1. Temperature and relative humidity

At present, the effects of temperature and RH on the decay of viral activity are a concern of most studies. Temperature can affect the infectivity of viruses by affecting the stability of the proteins, lipids, and genetic materials that make up the virus [4,15]. Correlation analysis showed that there was a significant negative correlation between temperature (4 °C–55 °C) and half-life ($\log_{10}$ of $Rt_{1/2}$) for SARS-CoV-2 and influenza viruses (Pearson's $r = 0.57$ and Pearson's $r = 0.59$, $p < 0.05$) (Fig. 3). Notably, coronavirus has stronger resistance to inactivation by temperature than other respiratory viruses on the surfaces, showing a higher $Rt_{1/2}$ at 20 °C–30 °C; increasing protein content in suspensions could generally improve the estimated $Rt_{1/2}$ of SARS-CoV-2 and influenza viruses on surfaces (Table S4). As shown in Fig. 3a and 3c, the values of $Rt_{1/2}$ were higher in the culture medium containing higher fetal bovine serum (protein content) at 20 °C–30 °C.

Here, we mainly review the latest research on viral infectivity in aerosols (Table 1). The types or subtypes of viruses may affect the viral sensitivity to temperature, but viral inactivation at high temperature is definite. The $Rt_{1/2}$ of SARS-CoV-2 in aerosols decreased from 11.55 h to 0.40 h when the temperature increased from 10 °C to 30 °C at 70% RH [124]. Similarly, nebulized HCoV-229E can survive with an $Rt_{1/2}$ of 67.33 h at 20 °C/50% RH and has higher stability at 6 °C/50% RH ($Rt_{1/2}$ of 102.53 h) [125].

The effect of RH on viral infectivity and its mechanism are still debateable. At present, we cannot find a significant correlation between the RH and the half-lives of the viruses (Fig. 3). For example, at 20 °C, the infectivity of rhinovirus in aerosols is rapidly lost at low and medium RH, while it is highly stable at high RH with a half-life of 13.7 h [44,62]. Some studies reported maximum decay of influenza viruses in aerosols at moderate RH (50%–70% RH) [41,126], while others reported maximum decay at high RH (~80% RH) [45,127]. Recent studies have shown

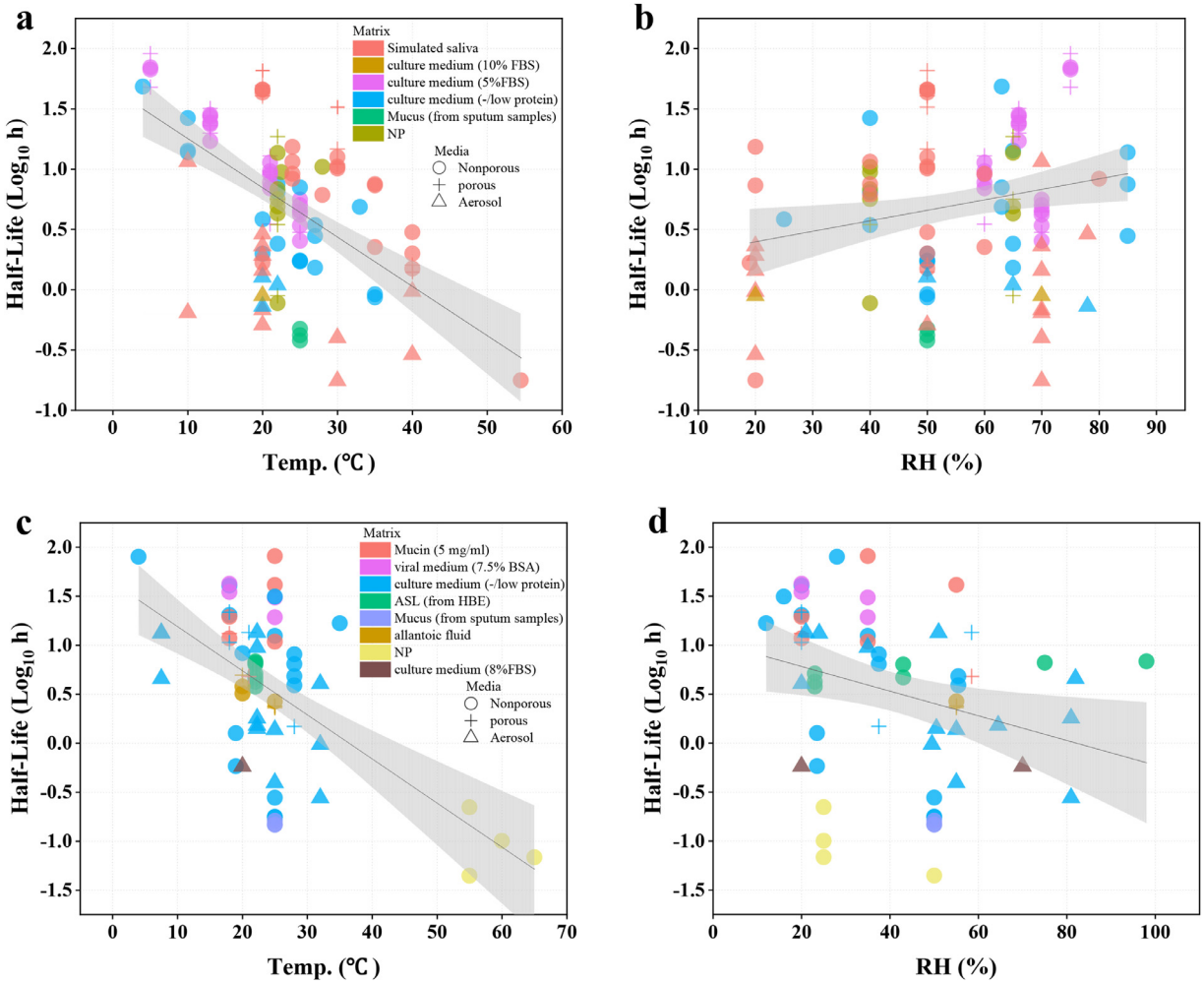

Fig. 3. The relationship between the half-lives of viruses and temperature as well as RH according to the papers reviewed in this article. (a) The half-life (log_{10} h) of SARS-CoV-2 vs. temperature. (b) SARS-CoV-2 vs. RH. (c) Influenza virus vs. temperature. (d) Influenza viruses vs. RH. (a) and (b) share the same legend; (c) and (d) share the same legend. Color represents the difference in suspension composition. Different shapes represent the difference in media: circles and crosses show the studies on viruses deposited on nonporous and porous surfaces, respectively, and triangles show the studies on viruses in aerosols.

that the addition of proteins such as fetal bovine serum, mucin, or extracellular substances to the virus suspension could reduce or eliminate the decay of viral infectivity in aerosols caused by RH [29,50,85]. Smither et al. [26] noted that the difference in components of suspensions could lead to the different sensitivities of infectious SARS-CoV-2 to RH.

To explore the mechanism of RH on viral infectivity, some scientists have made assumptions based on the evaporation kinetics of droplets [105,128]. Using dual-balance quadrupole electrodynamic balance technology (DBQ-EDB), Huynh et al. [129] studied the phase transition of aerosols induced by RH and proposed that the organic semisolid state of particles under RH (45%–80%) protected the pathogens from inactivation and that higher protein content caused the particles to exist as a semisolid under the condition of higher RH. Morris et al. [104] developed a mechanistic biochemical mode of inactivation of the virus on surfaces Eq. 3 and explained the U-shaped dependence between the infectivity of SARS-CoV-2 and RH. This mechanistic model was used to predict the half-lives of five human coronaviruses containing SARS-CoV-2, SARS-CoV-1, MERS-CoV, HCoV-229E, and HCoV-OC43, and the predictions effectively matched the measurements.

$$k_{eff} = A_{eff} \exp\left(-\frac{E_a}{RT}\right)$$
$$k_{sol} = \frac{[S_{eq}]}{[S_0]} A_{sol} \exp\left(-\frac{E_a}{RT}\right) \quad (3)$$

However, this model may not be suitable to explain the effect of RH on viral infectivity in aerosols. Under different RHs, the components and concentrations of the suspensions affect the size and composition of aerosol particles, thus affecting sedimentation and inactivation of the virus.

4.2. Sunlight radiation

Ultraviolet C (UVC, wavelengths 100–280 nm) radiation has been widely studied and proven to be effective against various viruses [130]. However, UVC from the sun is unable to penetrate the Earth's atmosphere. Most of the UV radiation that reaches the Earth's surface is UVA (315–400 nm) with a small amount of UVB (280–315 nm). Many studies have reported that UVA does not inactivate viruses suspended in solution, while UVB has a certain effect on infectious decay [15,131].

Table 3 summarizes the half-lives of viral infectivity in aerosols and on surfaces under different intensities of simulated sunlight. The related studies are mainly from the National Biodefense Analysis and Countermeasures Center (NBACC), USA. They found that simulated sunlight could effectively increase the decay of viral infectivity. Specifically, the half-life of influenza viruses in aerosols was 31.6 min ($Rt_{1/2}$ = 34.7 min) at 20 °C and darkness; however, under the conditions of high sunlight intensity (52.86 W/m^2 UVA and 1.44 W/m^2 UVB) simulating sunny

Table 3
Summary of the laboratory studies on the half-lives of viral aerosols under simulated sunlight.

Virus	Matrix	Temperature (°C)	RH (%)	irradiance	$Rt_{1/2}$ (min)	Reference
Aerosol						
SARS-CoV-2	Simulated respiratory tract lining fluid	10–40	20–70	0	24–693	Schuit et al. [124]
		10–30	20–70	69.76 W/m^2 UVA; 1.91 W/m^2 UVB	2.4–5.98	
		20	45	31.97 W/m^2 UVA; 0.94 W/m^2 UVB	4.47	
SARS-CoV-2	Simulated saliva	10–40	20, 70	0	10.8–>115.8	Dabisch et al. [49]
		10–30	45	0.9 W/m^2 UVB	3.47–5.87	
		10–40	20, 70	1.9 W/m^2 UVB	1.42–3.29	
SARS-CoV-2	Simulated saliva	20	20–70	0	86.64	Schuit et al. [47]
		20	20–70	31.97 W/m^2 UVA; 0.94 W/m^2 UVB	5.73	
		20	20–70	69.76 W/m^2 UVA; 1.91 W/m^2 UVB	2.27	
	culture medium (10% FBS)	20	20–70	0	53.32	
		20	20–70	31.97 W/m^2 UVA; 0.94 W/m^2 UVB	4.10	
		20	20–70	69.76 W/m^2 UVA; 1.91 W/m^2 UVB	3.81	
Influenza A virus	culture medium (8% FBS)	20	20, 70	0	34.66	Schuit et al. [50]
		20	20, 70	24.48 W/m^2 UVA; 0.62 W/m^2 UVB	4.05	
		20	20, 70	52.86 W/m^2 UVA; 1.44 W/m^2 UVB	2.39	
Surface						
SARS-CoV-2	culture medium (5% FBS)	20	–	3000 lux visible light	158.58	Uema et al. [132]
SARS-CoV-2	culture medium (1% BCS)	22.5	34	0	301.03	Sloan et al. [89]
		22.5	34	41.46 W/m^2 UVA; 1.28 W/m^2 UVB	6.84	
	simulated mucus	22.5	34	0	100.34	
		22.5	34	41.46 W/m^2 UVA; 1.28 W/m^2 UVB	27.37	
	culture medium (1% BCS)	25–34	29–41	0	43.00	
		25–34	29–41	41.46 W/m^2 UVA; 1.28 W/m^2 UVB	8.85	
	simulated mucus	25–34	24–41	0	150.51	
		25–34	24–41	41.46 W/m^2 UVA; 1.28 W/m^2 UVB	20.07	
SARS-CoV-2	DMEM	20–35	50	0	55.01–119.51	Raiteux et al. [94]
		20–35	50	79 W/m^2 UVA+UVB	2.72–3.04	
		35	50	442 W/m^2 UVA+UVB	0.65	
	DMEM (1% BSA + 1% yeast extract)	35	50	0	51.73	
		35	50	442 W/m^2 UVA+UVB	0.74	
SARS-CoV-2	Simulated saliva	20	19	0	100.34	Ratnesar-Shumate et al. [95]
		20	19	0.3 W/m^2 UVB	3.86	
		20	19	0.7 W/m^2 UVB	2.41	
		20	19	1.6 W/m^2 UVB	2.03	
	culture medium (10% FBS)	20	19	0.3 W/m^2 UVB	16.72	
		20	19	0.7 W/m^2 UVB	5.28	
		20	19	1.6 W/m^2 UVB	4.30	

weather at northern latitudes at 40 °C, the half-life of influenza viruses in aerosols was approximately 2.4 min, and viral decay increased with increasing exposure time and light intensity [50]. Under simulated sunlight for late winter/early autumn (31.97 W/m^2 UVA and 0.94 W/m^2 UVB) and summer (69.76 W/m^2 UVA and 1.91 W/m^2 UVB), the half-lives of SARS-CoV-2 were only 5.7 min and 2.3 min, respectively [47]. Similarly, SARS-CoV-2 deposited on surfaces is also affected by sunlight. Under different UVB intensities (0.3, 0.7, 1.6 W/m^2 UVB), a ninety percent loss of the virus took only 6.8–55.6 min, equivalent to a half-life of 2–16 min, which was much lower than that in dark conditions (at least 100 min of $Rt_{1/2}$) [95]. However, Uema et al. [132] found that visible light does not inactivate viruses as endogenously as UVB does. The effect of solar radiation in the ambient air on the infectivity of respiratory viruses remains unknown.

4.3. Ozone

Ozone, as an effective gas disinfectant, has been widely used to inactivate a variety of microorganisms and viruses. Recently, Farooq and Tizaoui [19] reviewed the research status of ozone disinfection of SARS-CoV-2 on surfaces and in the air. They noted that at 60%–99% RH and ambient temperature, 99% of SARS-CoV-2 adhered to common surfaces could be inactivated within 60 min by 10–20,000 mg/m^3 ozone, while inactivation in aerosols needed less than 10 min at a lower ozone exposure of 2–10 mg/m^3. However, the level of O_3 used in these studies was much higher than that in ambient air.

At present, only a few studies have focused on the stability of infectious viruses on the surface and in aerosols under O_3 at ambient levels. For example, SARS-CoV-2 deposited on stainless steel could be reduced by ~95% after 10 h and 20 h of ozone exposure at 0.1 ppm and 0.05 ppm, respectively [133]. The copies of SARS-CoV-2 RNA (based on ICC-qPCR detection) significantly decreased (95.9%–97.7% loss) when exposed to high ambient ozone concentrations (250 μg/m^3) for 30 and 60 min [134]. Criscuolo et al. [135] showed that > 99.9% of the viral titre of SARS-CoV-2 in fleece could be lost after exposure to 0.2 ppm ozone for 2 h, while the reduction in viral infectivity on other materials was less significant (96.8% in gauze, 93.3% in wood, 90% in glass, and 82.2% in plastic). Ambient O_3 had a certain inactivation effect on viral infectivity, but its ability to inactivate needs to be further investigated because of the lack of unambiguous evidence.

5. Conclusion and outlook

Laboratory simulation studies under controlled environmental conditions are used to explore the survival and decay of infectious viruses. However, the simulation methods from aerosol generation, ageing, and sampling to detection of infectivity may change the results on the stability of the viruses. Several important experimental conditions, especially virus types, suspension components, inoculum load, and evaporation, have been found to be the main factors affecting the decay of infectious viruses. Presently, there are conflicting outcomes among the laboratory studies. The experimental methods need to be standardized to minimize and quantify their effects on the damage of infectivity, in order to produce more comparable experimental results among the different studies. In addition, sampling technologies to maximize biological recovery and

detection methods with high time resolution and sensitivity need to be further developed and applied.

Damage to viral infectivity in the artificial generation of aerosols is not conducive to study the impact of the environmental factors on the virus transmission and to conduct long-term observations due to the lack of viruses with high titres. Therefore, the mechanism by which the characteristics of exhaled aerosols affect viral infectivity is not clear. Chemical composition, evaporation rate, phase change and pH may be several key parameters. Single-particle observation and quantitative analysis of aerosols may promote studies on droplet microenvironments.

Laboratory studies have shown that under simulated atmospheric conditions, the half-lives of respiratory viruses range from a few minutes to several hours. According to existing laboratory studies, the viruses in aerosols have lower half-lives than those on surfaces. An increasing number of studies have focused on the effects of atmospheric environmental conditions on viral infectivity in aerosols, but most have only focused on the temperature and RH. From the results of the half-lives of the viruses, sunlight (mainly UVB) has a significant impact, but few studies on this have been performed. The mechanism by which other atmospheric conditions and atmospheric pollutants (O_3, SO_2, and NO_2) affect the decay of infectious viruses remains elusive. The effects of the interactions of various factors at ambient dose on viral infectivity need to also be considered to better match real world situations. Furthermore, the sensitivity of different variants of influenza viruses and coronaviruses to the atmospheric environment is still very unclear. All of these aspects warrant future laboratory studies.

Declaration of competing interest

The authors declare that they have no conflicts of interest in this work.

Acknowledgments

This work was supported by the National Natural Science Foundation of China (42130611) and Guangdong Foundation for Program of Science and Technology Research (2023B1212060049, 2019B121205006).

Supplementary materials

Supplementary material associated with this article can be found, in the online version, at doi:10.1016/j.fmre.2023.12.017.

References

[1] C. Troeger, B.F. Blacker, I.A. Khalil, et al., Estimates of the global, regional, and national morbidity, mortality, and aetiologies of lower respiratory infections in 195 countries, 1990-2016: A systematic analysis for the Global Burden of Disease Study 2016, Lancet Infectious Dis. 18 (2018) 1191–1210.
[2] A.D. Iuliano, K.M. Roguski, H.H. Chang, et al., Estimates of global seasonal influenza-associated respiratory mortality: A modelling study, Lancet 391 (2018) 1285–1300.
[3] C. Sohrabi, Z. Alsafi, N. O'Neill, et al., World Health Organization declares global emergency: A review of the 2019 Novel Coronavirus (COVID-19), Int. J. Surg. 76 (2020) 71–76.
[4] C.C. Wang, K.A. Prather, J. Sznitman, et al., Airborne transmission of respiratory viruses, Science (1979) 373 (2021) eabd9149.
[5] I.T.S. Yu, Y.G. Li, T.W. Wong, et al., Evidence of airborne transmission of the severe acute respiratory syndrome virus, N. Engl. J. Med. 350 (2004) 1731–1739.
[6] S.-H. Kim, S.Y. Chang, M. Sung, et al., Extensive viable Middle East respiratory syndrome (MERS) coronavirus contamination in air and surrounding environment in MERS Isolation wards, Clin. Infect. Dis. 63 (2016) 363–369.
[7] T.F. Booth, B. Kournikakis, N. Bastien, et al., Detection of airborne severe acute respiratory syndrome (SARS) coronavirus and environmental contamination in SARS outbreak units, J. Infect. Dis. 191 (2005) 1472–1477.
[8] N.H.L. Leung, D.K.W. Chu, E.Y.C. Shiu, et al., Respiratory virus shedding in exhaled breath and efficacy of face masks, Nat. Med. 26 (2020) 676–680.
[9] World Health Organization. (2020). Transmission of SARS-CoV-2: Implications for infection prevention precautions: Scientific brief, 09 July 2020. Retrieved from Geneva: https://apps.who.int/iris/handle/10665/333114
[10] M.S. Yao, L. Zhang, J.X. Ma, et al., On airborne transmission and control of SARS–CoV-2, Sci. Total Environ. 731 (2020) 139178.
[11] W. Sun, X.D. Hu, Y.H. Hu, et al., Influence of atmospheric environment on SARS–CoV-2 transmission: A review Science bulletin (in Chinese) 67 (2022) 2509–2521.
[12] J.D. Tamerius, J. Shaman, W.J. Alonso, et al., Environmental predictors of seasonal influenza epidemics across temperate and tropical climates, PLoS. Pathog. 9 (2013) e1003194.
[13] T. Hong, P.L. Gurian, Y. Huang, et al., Prioritizing risks and uncertainties from intentional release of selected Category A pathogens, PLoS. One 7 (2012) e32732.
[14] M. Fernández-Raga, L. Díaz-Marugán, M. García Escolano, et al., SARS-CoV-2 viability under different meteorological conditions, surfaces, fluids and transmission between animals, Environ. Res. 192 (2021) 110293.
[15] H.A. Aboubakr, T.A. Sharafeldin, S.M. Goyal, Stability of SARS-CoV-2 and other coronaviruses in the environment and on common touch surfaces and the influence of climatic conditions: A review, Transboundary Emerging Dis 68 (2021) 296–312.
[16] T.P. Weber, N.I. Stilianakis, Inactivation of influenza A viruses in the environment and modes of transmission: A critical review, J. Infect. Dis. 57 (2008) 361–373.
[17] M. Marques, J.L. Domingo, Contamination of inert surfaces by SARS-CoV-2: persistence, stability and infectivity. A review, Environ. Res. 193 (2021) 110559.
[18] P.G. da Silva, M.S.J. Nascimento, R.R.G. Soares, et al., Airborne spread of infectious SARS-CoV-2: Moving forward using lessons from SARS-CoV and MERS-CoV, Sci. Total Environ. 764 (2021) 142802.
[19] S. Farooq, C. Tizaoui, A critical review on the inactivation of surface and airborne SARS-CoV-2 virus by ozone gas, Crit. Rev. Environ. Sci. Technol. 53 (2022) 87–109.
[20] D. Verreault, S. Moineau, C. Duchaine, Methods for sampling of airborne viruses, Mol. Biol. Rev. 72 (2008) 413–444.
[21] M.H. Pan, J.A. Lednicky, C.-Y. Wu, Collection, particle sizing and detection of airborne viruses, J. Appl. Microbiol. 127 (2019) 1596–1611.
[22] J.R. Brown, J.W. Tang, L. Pankhurst, et al., Influenza virus survival in aerosols and estimates of viable virus loss resulting from aerosolization and air-sampling, J. Hosp. Infect. 91 (2015) 278–281.
[23] N. Turgeon, M.-J. Toulouse, B. Martel, et al., Comparison of five bacteriophages as models for viral aerosol studies, Appl. Environ. Microbiol. 80 (2014) 4242–4250.
[24] S.G. Danelli, M. Brunoldi, D. Massabò, et al., Comparative characterization of bio-aerosol nebulizers in connection to atmospheric simulation chambers, Atmos. Meas. Tech. 14 (2021) 4461–4470.
[25] A.C. Fears, W.B. Klimstra, P. Duprex, et al., Persistence of severe acute respiratory syndrome coronavirus 2 in aerosol suspensions, Emerging Infect. Dis. 26 (2020) 2168–2171.
[26] S.J. Smither, L.S. Eastaugh, J.S. Findlay, et al., Experimental aerosol survival of SARS-CoV-2 in artificial saliva and tissue culture media at medium and high humidity, Emerging Microbes Infect 9 (2020) 1415–1417.
[27] O.V. Pyankov, S.A. Bodnev, O.G. Pyankova, et al., Survival of aerosolized coronavirus in the ambient air, J. Aerosol Sci. 115 (2018) 158–163.
[28] O.V. Pyankov, O.G. Pyankova, I.E. Agranovski, Inactivation of airborne influenza virus in the ambient air, J. Aerosol Sci. 53 (2012) 21–28.
[29] K.A. Kormuth, K. Lin, A.J. Prussin II, et al., Influenza virus infectivity is retained in aerosols and droplets independent of relative humidity, J. Infect. Dis. 218 (2018) 739–747.
[30] S. Niazi, L.K. Philp, K. Spann, et al., Utility of three nebulizers in investigating the infectivity of airborne viruses, Appl. Environ. Microbiol. 87 (2021) e00497 00421.
[31] L. Zupin, S. Licen, M. Milani, et al., Evaluation of residual infectivity after SARS–CoV-2 aerosol transmission in a controlled laboratory setting, Int. J. Environ. Res. Public Health 18 (2021) 11172.
[32] Z. Zuo, H. Kuehn Thomas, Z. Bekele Aschalew, et al., Survival of airborne MS2 bacteriophage generated from human saliva, artificial saliva, and cell culture medium, Appl. Environ. Microbiol. 80 (2014) 2796–2803.
[33] M.-E. Dubuis, É. Racine, J.M. Vyskocil, et al., Ozone inactivation of airborne influenza and lack of resistance of respiratory syncytial virus to aerosolization and sampling processes, PLoS. One 16 (2021) e0253022.
[34] K.M. Gustin, J.A. Belser, V. Veguilla, et al., Environmental conditions affect exhalation of H3N2 seasonal and variant influenza viruses and respiratory droplet transmission in ferrets, PLoS. One 10 (2015) e0125874.
[35] W. Yang, L.C. Marr, Dynamics of airborne influenza A viruses indoors and dependence on humidity, PLoS. One 6 (2011) e21481.
[36] J.D. Noti, F.M. Blachere, C.M. McMillen, et al., High humidity leads to loss of infectious influenza virus from simulated coughs, PLoS. One 8 (2013) e57485.
[37] M.L. Pöhlker, O.O. Krüger, J.-D. Förster, et al., Respiratory aerosols and droplets in the transmission of infectious diseases, arXiv:2103.01188 [physics.med-ph] (2021). https://doi.org/10.48550/arXiv.2103.01188
[38] W. Yang, L.C. Marr, Mechanisms by which ambient humidity may affect viruses in aerosols, Appl. Environ. Microbiol. 78 (2012) 6781–6788.
[39] J.L. Santarpia, S. Ratnesar-Shumate, A. Haddrell, Laboratory study of bioaerosols: Traditional test systems, modern approaches, and environmental control, Aerosol Sci. Technol. 54 (2019) 585–600.
[40] A.E. Haddrell, R.J. Thomas, Aerobiology: Experimental considerations, observations, and future tools, Appl. Environ. Microbiol. 83 (2017) e00809–e00817.
[41] F.L. Schaffer, M.E. Soergel, D.C. Straube, Survival of airborne influenza virus: effects of propagating host, relative humidity, and composition of spray fluids, Arch. Virol. 51 (1976) 263–273.
[42] M. Dybwad, G. Skogan, J.M. Blatny, Comparative testing and evaluation of nine different air samplers: End-to-end sampling efficiencies as specific performance measurements for bioaerosol applications, Aerosol Sci. Technol. 48 (2014) 282–295.
[43] S. Ratnesar-Shumate, K. Bohannon, G. Williams, et al., Comparison of the performance of aerosol sampling devices for measuring infectious SARS-CoV-2 aerosols, Aerosol Sci. Technol. 55 (2021) 975–986.
[44] Y.G. Karim, M.K. Ijaz, S.A. Sattar, et al., Effect of relative humidity on the airborne survival of rhinovirus-14, Can. J. Microbiol. 31 (1985) 1058–1061.

[45] G.J. Harper, Airborne micro-organisms: Survival tests with four viruses, Epidemiol. Infect. 59 (1961) 479–486.
[46] J. Rechsteiner, K.C. Winkler, Inactivation of respiratory syncytial virus in aerosol, J. Gen. Virol. 5 (1969) 405–410.
[47] M. Schuit, S. Ratnesar-Shumate, J. Yolitz, et al., Airborne SARS-CoV-2 is rapidly inactivated by simulated sunlight, J. Infect. Dis. 222 (2020) 564–571.
[48] S.-H. Huang, Y.-M. Kuo, C.-W. Lin, et al., Experimental characterization of aerosol suspension in a rotating drum, Aerosol Air Qual. Res. 19 (2019) 688–697.
[49] P. Dabisch, M. Schuit, A. Herzog, et al., The influence of temperature, humidity, and simulated sunlight on the infectivity of SARS-CoV-2 in aerosols, Aerosol Sci. Technol. 55 (2021) 142–153.
[50] M. Schuit, S. Gardner, S. Wood, et al., The influence of simulated sunlight on the inactivation of influenza virus in aerosols, J. Infect. Dis. 221 (2019) 372–378.
[51] T.M. Cruz-Sanchez, A.E. Haddrell, T.L. Hackett, et al., Formation of a stable mimic of ambient particulate matter containing viable infectious respiratory syncytial virus and its dry-deposition directly onto cell cultures, Anal. Chem. 85 (2013) 898–906.
[52] M.O. Fernandez, R.J. Thomas, N.J. Garton, et al., Assessing the airborne survival of bacteria in populations of aerosol droplets with a novel technology, J. R. Soc. Interface 16 (2019) 20180779.
[53] H.P. Oswin, A.E. Haddrell, M. Otero-Fernandez, et al., Measuring stability of virus in aerosols under varying environmental conditions, Aerosol Sci. Technol. 55 (2021) 1315–1320.
[54] G. Mainelis, Bioaerosol sampling: Classical approaches, advances, and perspectives, Aerosol Sci. Technol. 54 (2020) 496–519.
[55] J. Bhardwaj, S. Hong, J. Jang, et al., Recent advancements in the measurement of pathogenic airborne viruses, J. Hazard. Mater. 420 (2021) 126574.
[56] J.A. Lednicky, J.C. Loeb, Detection and isolation of airborne influenza A H3N2 virus using a Sioutas Personal Cascade Impactor Sampler, Influenza Res. Treat. 2013 (2013) 656825.
[57] W.G. Lindsley, D. Schmechel, B.T. Chen, A two-stage cyclone using microcentrifuge tubes for personal bioaerosol sampling, J. Environ. Monit. 8 (2006) 1136–1142.
[58] J.D. Noti, W.G. Lindsley, F.M. Blachere, et al., Detection of infectious influenza virus in cough aerosols generated in a simulated patient examination room, Clin. Infect. Dis. 54 (2012) 1569–1577.
[59] W.B. Vass, J.A. Lednicky, S.N. Shankar, et al., Viable SARS-CoV-2 Delta variant detected in aerosols in a residential setting with a self-isolating college student with COVID-19, J. Aerosol Sci. 165 (2022) 106038.
[60] G. Cao, J.D. Noti, F.M. Blachere, et al., Development of an improved methodology to detect infectious airborne influenza virus using the NIOSH bioaerosol sampler, J. Environ. Monit. 13 (2011) 3321–3328.
[61] N. van Doremalen, T. Bushmaker, V.J. Munster, Stability of Middle East respiratory syndrome coronavirus (MERS-CoV) under different environmental conditions, Euro. Surveill. 18 (2013) 20590.
[62] M.K. Ijaz, Y.G. Karim, S.A. Sattar, et al., Development of methods to study the survival of airborne viruses, J. Virol. Methods 18 (1987) 87–106.
[63] W.G. Lindsley, F.M. Blachere, D.H. Beezhold, et al., Viable influenza A virus in airborne particles expelled during coughs versus exhalations, Influenza Other Respir, Viruses. 10 (2016) 404–413.
[64] M.H. Pan, S. Bonny Tania, J. Loeb, et al., Collection of viable aerosolized influenza virus and other respiratory viruses in a student health care center through water-based condensation growth, mSphere 2 (2017) e00251 00217.
[65] P. Fabian, J.J. McDevitt, E.A. Houseman, et al., Airborne influenza virus detection with four aerosol samplers using molecular and infectivity assays: Considerations for a new infectious virus aerosol sampler, Indoor. Air. 19 (2009) 433–441.
[66] C.J. Hogan Jr, E.M. Kettleson, M.H. Lee, et al., Sampling methodologies and dosage assessment techniques for submicrometre and ultrafine virus aerosol particles, J. Appl. Microbiol. 99 (2005) 1422–1434.
[67] J.Y. Li, A. Leavey, Y. Wang, et al., Comparing the performance of 3 bioaerosol samplers for influenza virus, J. Aerosol Sci. 115 (2018) 133–145.
[68] N.C. Burton, S.A. Grinshpun, T. Reponen, Physical collection efficiency of filter materials for bacteria and viruses, Ann. Occup. Hyg. 51 (2007) 143–151.
[69] J.S. Kutter, D. de Meulder, T.M. Bestebroer, et al., Comparison of three air samplers for the collection of four nebulized respiratory viruses - Collection of respiratory viruses from air, Indoor. Air. 31 (2021) 1874–1885.
[70] J.L. Santarpia, D.N. Rivera, V.L. Herrera, et al., Aerosol and surface contamination of SARS-CoV-2 observed in quarantine and isolation care, Sci. Rep. 10 (2020) 12732.
[71] N. Dumont-Leblond, M. Veillette, S. Mubareka, et al., Low incidence of airborne SARS-CoV-2 in acute care hospital rooms with optimized ventilation, Emerg. Microbes Infect. 9 (2020) 2597–2605.
[72] M.H. Pan, A. Eiguren-Fernandez, H. Hsieh, et al., Efficient collection of viable virus aerosol through laminar-flow, water-based condensational particle growth, J. Appl. Microbiol. 120 (2016) 805–815.
[73] J. Lednicky, M.H. Pan, J. Loeb, et al., Highly efficient collection of infectious pandemic influenza H1N1 virus (2009) through laminar-flow water based condensation, Aerosol Sci. Technol. 50 (2016) I–IV.
[74] S. Hong, J. Bhardwaj, C.-H. Han, et al., Gentle sampling of submicrometer airborne virus particles using a personal electrostatic particle concentrator, Environ. Sci. Technol. 50 (2016) 12365–12372.
[75] N.R. de Sousa, L. Steponaviciute, L. Margerie, et al., Detection and isolation of airborne SARS-CoV-2 in a hospital setting, Indoor. Air. 32 (2022) e13023.
[76] A. Piri, H.R. Kim, D.H. Park, et al., Increased survivability of coronavirus and H1N1 influenza virus under electrostatic aerosol-to-hydrosol sampling, J. Hazard. Mater. 413 (2021) 125417.
[77] Z.G. Ke, P. Thopan, G. Fridman, et al., Effect of N2/O2 composition on inactivation efficiency of Escherichia coli by discharge plasma at the gas-solution interface, Clin. Plasma Med. 7-8 (2017) 1–8.
[78] R. Hirose, H. Ikegaya, Y. Naito, et al., Survival of severe acute respiratory syndrome coronavirus 2 (SARS-CoV-2) and influenza virus on human skin: Importance of hand hygiene in Coronavirus Disease 2019 (COVID-19), Clin. Infect. Dis. 73 (2021) e4329–e4335.
[79] N. van Doremalen, T. Bushmaker, D.H. Morris, et al., Aerosol and surface stability of SARS-CoV-2 as compared with SARS-CoV-1, N. Engl. J. Med. 382 (2020) 1564–1567.
[80] K.-H. Chan, S. Sridhar, R.R. Zhang, et al., Factors affecting stability and infectivity of SARS-CoV-2, J. Hosp. Infect. 106 (2020) 226–231.
[81] H.F. Rabenau, J. Cinatl, B. Morgenstern, et al., Stability and inactivation of SARS coronavirus, Med. Microbiol. Immunol. 194 (2005) 1–6.
[82] J. Sizun, M.W.N. Yu, P.J. Talbot, Survival of human coronaviruses 229E and OC43 in suspension and after drying on surfaces: A possible source of hospital-acquired infections, J. Hosp. Infect. 46 (2000) 55–60.
[83] Y. Thomas, G. Vogel, W. Wunderli, et al., Survival of influenza virus on banknotes, Appl. Environ. Microbiol. 74 (2008) 3002–3007.
[84] B. Bean, B.M. Moore, B. Sterner, et al., Survival of influenza viruses on environmental surfaces, J. Infect. Dis. 146 (1982) 47–51.
[85] K.A. Kormuth, K.S. Lin, Z.H. Qian, et al., Environmental persistence of influenza viruses is dependent upon virus type and host origin, mSphere 4 (2019) e00552-19.
[86] K.A. Perry, A.D. Coulliette, L.J. Rose, et al., Persistence of influenza A (H1N1) virus on stainless steel surfaces, Appl. Environ. Microbiol 82 (2016) 3239–3245.
[87] E.R. Parker, W.B. Dunham, W.J. MacNeal, Resistance of the Melbourne strain of influenza virus to desiccation, J. Lab. Clin. Med. 29 (1944) 37–42.
[88] W. Yang, S. Elankumaran, L.C. Marr, Relationship between humidity and influenza A viability in droplets and implications for influenza's seasonality, PLoS. One 7 (2012) e46789.
[89] A. Sloan, T. Cutts, B.D. Griffin, et al., Simulated sunlight decreases the viability of SARS-CoV-2 in mucus, PLoS. One 16 (2021) e0253068.
[90] J. Biryukov, J.A. Boydston, R.A. Dunning, et al., SARS-CoV-2 is rapidly inactivated at high temperature, Environ. Chem. Lett. 19 (2021) 1773–1777.
[91] S. Riddell, S. Goldie, A. Hill, et al., The effect of temperature on persistence of SARS-CoV-2 on common surfaces, Virol. J. 17 (2020) 145.
[92] J. Biryukov, J.A. Boydston, R.A. Dunning, et al., Increasing temperature and relative humidity accelerates inactivation of SARS-CoV-2 on surfaces, mSphere 5 (2020) e00441 00420.
[93] B. Pastorino, F. Touret, M. Gilles, et al., Prolonged infectivity of SARS-CoV-2 in fomites, Emerging Infect. Dis. 26 (2020) 2256–2257.
[94] J. Raiteux, M. Eschlimann, A. Marangon, et al., Inactivation of SARS-CoV-2 by simulated sunlight on contaminated surfaces, Microbiol. Spectrum 9 (2021) e00333 00321.
[95] S. Ratnesar-Shumate, G. Williams, B. Green, et al., Simulated sunlight rapidly inactivates SARS-CoV-2 on surfaces, J. Infect. Dis. 222 (2020) 214–222.
[96] Y. Thomas, P. Boquete-Suter, D. Koch, et al., Survival of influenza virus on human fingers, Clin. Microbiol. Infect. 20 (2014) O58–O64.
[97] A. French, A. Longest, J. Pan, et al., Environmental stability of enveloped viruses is impacted by initial volume and evaporation kinetics of droplets, mBio 14 (2023) e0345222.
[98] M.T. Brady, J. Evans, J. Cuartas, Survival and disinfection of parainfluenza viruses on environmental surfaces, Am. J. Infect. Control 18 (1990) 18–23.
[99] A.W.H. Chin, J.T.S. Chu, M.R.A. Perera, et al., Stability of SARS-CoV-2 in different environmental conditions, Lancet Microbe 1 (2020) E10.
[100] M.Y.Y. Lai, P.K.C. Cheng, W.W.L. Lim, Survival of severe acute respiratory syndrome coronavirus, Clin. Infect. Dis. 41 (2005) e67–e71.
[101] K.-H. Chan, J.S.M. Peiris, S.Y. Lam, et al., The effects of temperature and relative humidity on the viability of the SARS coronavirus, Adv. Virol. 2011 (2011) 734690.
[102] T. Kwon, N.N. Gaudreault, J.A. Richt, Environmental stability of SARS-CoV-2 on different types of surfaces under indoor and seasonal climate conditions, Pathogens. 10 (2021) 227.
[103] S. Firquet, S. Beaujard, P.-E. Lobert, et al., Survival of enveloped and non-enveloped viruses on inanimate surfaces, Microbes. Environ. 30 (2015) 140–144.
[104] D.H. Morris, K.C. Yinda, A. Gamble, et al., Mechanistic theory predicts the effects of temperature and humidity on inactivation of SARS-CoV-2 and other enveloped viruses, Elife 10 (2021) e65902.
[105] K.S. Lin, L.C. Marr, Humidity-dependent decay of viruses, but not bacteria, in aerosols and droplets follows disinfection kinetics, Environ. Sci. Technol. 54 (2020) 1024–1032.
[106] E. Percivalle, M. Clerici, I. Cassaniti, et al., SARS-CoV-2 viability on different surfaces after gaseous ozone treatment: A preliminary evaluation, J. Hosp. Infect. 110 (2021) 33–36.
[107] A. Dublineau, C. Batéjat, A. Pinon, et al., Persistence of the 2009 pandemic influenza A (H1N1) virus in water and on non-porous surface, PLoS. One 6 (2011) e28043.
[108] R. Dulbecco, Production of plaques in monolayer tissue cultures by single particles of an animal virus, Proc. Natl. Acad. Sci. U. S. A. 38 (1952) 747–752.
[109] V.I. Agol, Cytopathic effects: Virus-modulated manifestations of innate immunity? Trends. Microbiol. 20 (2012) 570–576.
[110] S.M. Duan, X.S. Zhao, R.F. Wen, et al., Stability of SARS coronavirus in human specimens and environment and its sensitivity to heating and UV irradiation, Biomed. Environ. Sci. 16 (2003) 246–255.
[111] S. Nuanualsuwan, D.O. Cliver, Pretreatment to avoid positive RT-PCR results with inactivated viruses, J. Virol. Methods 104 (2002) 217–225.
[112] L. Bonifait, R. Charlebois, A. Vimont, et al., Detection and quantification of airborne

norovirus during outbreaks in healthcare facilities, Clin. Infect. Dis. 61 (2015) 299–304.
[113] A. Carratalà, J. Rodriguez-Manzano, A. Hundesa, et al., Effect of temperature and sunlight on the stability of human adenoviruses and MS2 as fecal contaminants on fresh produce surfaces, Int. J. Food Microbiol. 164 (2013) 128–134.
[114] A. Cassedy, A. Parle-McDermott, R. O'Kennedy, Virus detection: A review of the current and emerging molecular and immunological methods, Front. Mol. Biosci. 8 (2021) 637559.
[115] A.I. Pimenta, D. Guerreiro, J. Madureira, et al., Tracking human adenovirus inactivation by gamma radiation under different environmental conditions, Appl. Environ. Microbiol. 82 (2016) 5166–5173.
[116] Y.X. Li, M. Hong, B. Qiu, et al., A highly sensitive chemiluminescent metalloimmunoassay for H1N1 influenza virus detection based on a silver nanoparticle label, Chem. Commun. 49 (2013) 10563–10565.
[117] M.S. Yao, SARS-CoV-2 aerosol transmission and detection, Eco-Environment & Health 1 (2022) 3–10.
[118] G. Seo, G. Lee, M.J. Kim, et al., Rapid detection of COVID-19 causative virus (SARS-CoV-2) in human nasopharyngeal swab specimens using field-effect transistor-based biosensor, ACS. Nano 14 (2020) 5135–5142.
[119] J.O. Noyce, H. Michels, C.W. Keevil, Inactivation of influenza A virus on copper versus stainless steel surfaces, Appl. Environ. Microbiol. 73 (2007) 2748–2750.
[120] S.T. Kazmer, G. Hartel, H. Robinson, et al., Pathophysiological response to SARS-CoV-2 infection detected by infrared spectroscopy enables rapid and robust saliva screening for COVID-19, Biomedicines. 10 (2022). https://doi.org/10.3390/biomedicines10020351.
[121] L. Zhan, S.J. Zhen, X.Y. Wan, et al., A sensitive surface-enhanced Raman scattering enzyme-catalyzed immunoassay of respiratory syncytial virus, Talanta 148 (2016) 308–312.
[122] Y.-T. Yeh, K. Gulino, Y. Zhang, et al., A rapid and label-free platform for virus capture and identification from clinical samples, Proc. Natl. Acad. Sci. U. S. A. 117 (2020) 895–901.
[123] L. Guillier, S. Martin-Latil, E. Chaix, et al., Modeling the inactivation of viruses from the Coronaviridae family in response to temperature and relative humidity in suspensions or on surfaces, Appl. Environ. Microbiol. 86 (2020) e01244 01220.
[124] M. Schuit, J. Biryukov, K. Beck, et al., The stability of an isolate of the SARS-CoV-2 B1.1.7 lineage in aerosols is similar to 3 earlier isolates, J. Infect. Dis. 224 (2021) 1641–1648.
[125] M.K. Ijaz, A.H. Brunner, S.A. Sattar, et al., Survival characteristics of airborne human coronavirus 229E, J. Gen. Virol. 66 (1985) 2743–2748.
[126] I.L. Shechmeister, Studies on the experimental epidemiology of respiratory infections: III. certain aspects of the behavior of Type A influenza virus as an air-borne cloud, J. Infect. Dis. 87 (1950) 128–132.
[127] J.H. Hemmes, K.C. Winkler, S.M. Kool, Virus survival as a seasonal factor in influenza and poliomyelitis, Nature 188 (1960) 430–431.
[128] L.C. Marr, J.W. Tang, J. Van Mullekom, et al., Mechanistic insights into the effect of humidity on airborne influenza virus survival, transmission and incidence, J. R. Soc. Interface 16 (2019) 20180298.
[129] E. Huynh, A. Olinger, D. Woolley, et al., Evidence for a semisolid phase state of aerosols and droplets relevant to the airborne and surface survival of pathogens, Proc. Natl. Acad. Sci. U. S. A. 119 (2022) e2109750119.
[130] D. Welch, M. Buonanno, I. Shuryak, et al., Far-UVC light applications: Sterilization of MRSA on a surface and inactivation of aerosolized influenza virus, Conference on Photonic Diagnosis and Treatment of Infections and Inflammatory Diseases at SPIE Photonics West BioSSan, 2018.
[131] K.L. Nelson, A.B. Boehm, R.J. Davies-Colley, et al., Sunlight-mediated inactivation of health-relevant microorganisms in water: a review of mechanisms and modeling approaches, Environ. Sci.-Proc. IMP 20 (2018) 1089–1122.
[132] M. Uema, K. Yonemitsu, Y. Momose, et al., Effect of the photocatalyst under visible light irradiation in SARS-CoV-2 stability on an abiotic surface, BioControl Sci. 26 (2021) 119–125.
[133] T. Murata, S. Komoto, S. Iwahori, et al., Reduction of severe acute respiratory syndrome coronavirus-2 infectivity by admissible concentration of ozone gas and water, Microbiol. Immunol. 65 (2021) 10–16.
[134] J. Cao, Y. Zhang, Q. Chen, et al., Ozone gas inhibits SARS-CoV-2 transmission and provides possible control measures, Aerosol Sci. Eng. 5 (2021) 516–523.
[135] E. Criscuolo, R.A. Diotti, R. Ferrarese, et al., Fast inactivation of SARS-CoV-2 by UV-C and ozone exposure on different materials, Emerg. Microbes Infect 10 (2021) 206–210.
[136] C. Rigotto, K. Hanley, P.A. Rochelle, et al., Survival of adenovirus types 2 and 41 in surface and ground waters measured by a plaque assay, Environ. Sci. Technol. 45 (2011) 4145–4150.
[137] Y. Liu, Z. Ning, Y. Chen, et al., Aerodynamic analysis of SARS-CoV-2 in two Wuhan hospitals, Nature 582 (2020) 557–560.
[138] J. Bhardwaj, M.-W. Kim, J. Jang, Rapid airborne influenza virus quantification using an antibody-based electrochemical paper sensor and electrostatic particle concentrator, Environ. Sci. Technol. 54 (2020) 10700–10712.
[139] R.A. Rodríguez, I.L. Pepper, C.P. Gerba, Application of PCR-based methods to assess the infectivity of enteric viruses in environmental samples, Appl. Environ. Microbiol. 75 (2009) 297–307.
[140] L.A. Layqah, S. Eissa, An electrochemical immunosensor for the corona virus associated with the Middle East respiratory syndrome using an array of gold nanoparticle-modified carbon electrodes, Microchim. Acta 186 (2019) 224.

Yaohao Hu is a Ph.D candidate at University of Chinese Academy of Sciences. His current research mainly focuses on the environmental stability of respiratory viruses during airborne transmission and the effect of atmospheric pollutants on the resistance to infection of respiratory viruses.

Xinhui Bi (BRID: 09118.00.31828) is currently a research professor at Guangzhou Institute of Geochemistry, Chinese Academy of Sciences. Her research areas mainly include in-cloud chemistry of secondary organic aerosols, aerosol evolution in ambient air, and health effects of air pollution.